# Large Acceleration Effect of Photoinduced Electron Transfer in Porphyrin−Quinone Dyads with a Rigid Spacer Involving a Dihalosubstituted Three-Membered Ring

**Hirohito Tsue,[‡] Hiroshi Imahori,*[,§] Takahiro Kaneda, Yoshinori Tanaka,[†] Tadashi Okada,*[,†] Koichi Tamaki, and Yoshiteru Sakata***

*Contribution from The Institute of Scientific and Industrial Research, Osaka University, Mihoga-oka, Ibaraki, Osaka 567-0047, Japan*

*Received January 4, 1999. Revised Manuscript Received November 30, 1999*

**Abstract:** To understand the contribution of spacer structure toward electron transfer (ET) and to regulate electronic coupling between a redox pair, porphyrin−spacer−benzoquinone molecules were prepared where spacers are *trans*-decalin and dihalosubstituted tricyclo[4.4.1.0]undecane including a three-membered ring. These compounds were designed to have almost the same separation distance between a redox pair, the same number of intervening bonds, and the nearly equal free energy change associated with the ET reaction. The ET rates for the charge separation process were evaluated on the basis of the fluorescence lifetimes. A quite large difference in the ET rates was observed among these compounds, and the ET rates for the compounds having the three-membered rings were ca. 50 to 60 times larger than that with *trans*-decalin spacer in THF. From the analysis of temperature dependence of the ET rates, it was shown that the observed rate acceleration is caused by both an increase of the electronic coupling and a decrease of the reorganization energy. Ab initio calculations of the electronic coupling elements and on molecular orbitals for the cyclopropanes predicted that the former may be due to the enhancement of the ET pathways arising from the bent geometry of the spacer or of the mixing pathway induced by a very low lying antibonding orbital in the dihalosubstituted cyclopropane.

## Introduction

To understand the mechanism of highly efficient forward electron transfer (ET) and retarded back ET in the primary process of photosynthesis, a number of synthetic models[1−26] have been reported. In most of the model compounds a donor and an acceptor are covalently connected with a flexible or a rigid spacer to eliminate the diffusion problem. Rigid spacers are much superior to flexible ones, since conformational complexity is excluded in the former case. By preparing (donor)−(rigid spacer)−(acceptor) systems, various controlling factors in ET such as separation distance, free energy change,

[†] Department of Chemistry, Graduate School of Engineering Science and Research Center for Materials Science at Extreme Conditions, Osaka University, Toyonaka, Osaka 560-8531, Japan.

[‡] Present address: Division of Material Science, Graduate School of Environmental Earth Science, Hokkaido University, Kita 10, Nishi 5, Kita-ku, Sapporo 060-0810, Japan.

[§] Present address: Department of Material and Life Science, Graduate School of Engineering, Osaka University, Suita, Osaka 565-0871, Japan.

(1) Connolly, J. S.; Bolton, J. R. In *Photoinduced Electron Transfer*; Fox, M. A., Chanon, M., Eds.; Elsevier: Amsterdam, 1988; Part D, pp 303−393.

(2) (a) Wasielewski, M. R. In *Photoinduced Electron Transfer*; Fox, M. A., Chanon, M., Eds.; Elsevier: Amsterdam, 1988; Part A, pp 161−206. (b) Wasielewski, M. R. *Chem. Rev.* **1992**, *92*, 435.

(3) (a) Gust, D.; Moore, T. A.; Moore, A. L. *Acc. Chem. Res.* **1993**, *26*, 198. (b) Maruyama, K.; Osuka, A.; Mataga, N. *Pure Appl. Chem.* **1994**, *66*, 867. (c) Kurreck, H.; Huber, M. *Angew. Chem., Int. Ed. Engl.* **1995**, *34*, 849. (d) Gust, D.; Moore, T. A.; Moore, A. L. *Res. Chem. Intermed.* **1997**, *23*, 621. (e) Imahori, H.; Sakata, Y. *Adv. Mater.* **1997**, *9*, 537. (f) Imahori, H.; Sakata, Y. *Eur. J. Org. Chem.* **1999**, 2445.

(4) (a) Joran, A. D.; Leland, B. A.; Geller, G. G.; Hopfield, J. J.; Dervan, P. B. *J. Am. Chem. Soc.* **1984**, *106*, 6090. (b) Leland, B. A.; Joran, A. D.; Felker, P. M.; Zewail, A. H.; Hopfield, J. J.; Dervan, P. B. *J. Phys. Chem.* **1985**, *89*, 5571. (c) Jordan, A. D.; Leland, B. A.; Felker, P. M.; Hopfield, J. J.; Zewail, A. H.; Dervan, P. B. *Nature* **1987**, *327*, 508. (d) Khundkar, L. R.; Perry, J. W.; Hanson, J. E.; Dervan, P. B. *J. Am. Chem. Soc.* **1994**, *116*, 9700.

(5) (a) Nishitani, S.; Kurata, N.; Sakata, Y.; Misumi, S.; Migita, M.; Okada, T.; Mataga, N. *Tetrahedron Lett.* **1981**, *22*, 2099. (b) Nishitani, S.; Kurata, N.; Sakata, Y.; Misumi, S.; Karen, A.; Okada, T.; Mataga, N. *J. Am. Chem. Soc.* **1983**, *105*, 7771. (c) Mataga, N.; Karen, A.; Okada, T.; Nishitani, S.; Kurata, N.; Sakata, Y.; Misumi, S. *J. Phys. Chem.* **1984**, *88*, 5138.

(6) (a) Kong, J. L. Y.; Loach, P. A. *J. Heterocycl. Chem.* **1980**, *17*, 737. (b) Kong, J. L. Y.; Spears, K. G.; Loach, P. A. *Photochem. Photobiol.* **1982**, *35*, 545.

(7) (a) Hush, N. S.; Paddon-Row, M. N.; Cotsaris, E.; Oevering, H.; Verhoeven, J. W.; Happener, M. *Chem. Phys. Lett.* **1985**, *117*, 8. (b) Oevering, H.; Paddon-Row, M. N.; Heppener, M.; Oliver, A. M.; Cotsaris, E.; Verhoeven, J. W.; Hush, N. S. *J. Am. Chem. Soc.* **1987**, *109*, 3258. (c) Penfield, K. W.; Miller, J. R.; Paddon-Row, M. N.; Cotsaris, E.; Oliver, A. M.; Hush, N. S. *J. Am. Chem. Soc.* **1987**, *109*, 5061. (d) Paddon-Row, M. N.; Verhoeven, J. W. *New J. Chem.* **1991**, *15*, 107.

(8) (a) Closs, G. L.; Calcaterra, L. T.; Green, N. J.; Penfield, K. W.; Miller, J. R. *J. Phys. Chem.* **1986**, *90*, 3673. (b) Johnson, M. D.; Miller, J. R.; Green, N. S.; Closs, G. L. *J. Phys. Chem.* **1989**, *93*, 1173.

(9) (a) Stein, C. A.; Taube, H. *J. Am. Chem. Soc.* **1978**, *100*, 1635. (b) Stein, C. A.; Taube, H. *J. Am. Chem. Soc.* **1981**, *103*, 693. (c) Stein, C. A.; Lewis, N. A.; Seitz, G. *J. Am. Chem. Soc.* **1982**, *104*, 2596. (d) Stein, C. A.; Lewis, N. A.; Seitz, G.; Baker, A. D. *Inorg. Chem.* **1983**, *22*, 1124. (e) Baker, A. D.; Sharfman, R.; Stein, C. A. *Tetrahedron Lett.* **1983**, *24*, 2957.

(10) (a) Miller, J. R.; Calcaterra, L. T.; Closs, G. L. *J. Am. Chem. Soc.* **1984**, *106*, 3047. (b) Closs, G. L.; Miller, J. R. *Science* **1988**, *240*, 440.

(11) Asahi, T.; Ohkohchi, M.; Matsusaka, R.; Mataga, N.; Zhang, R. P.; Osuka, A.; Maruyama, K. *J. Am. Chem. Soc.* **1993**, *115*, 5665.

(12) Wasielewski, M. R.; Niemczyk, M. P.; Svec, W. A.; Pewitt, E. B. *J. Am. Chem. Soc.* **1985**, *107*, 1080.

(13) Wasielewski, M. R.; Niemczyk, M. P.; Johnson, D. G.; Svec, W. A.; Minsek, D. W. *Tetrahedron* **1989**, *45*, 4785.

(14) Helms, A.; Heiler, D.; McLendon, G. *J. Am. Chem. Soc.* **1991**, *113*, 4325.

(15) Osuka, A.; Maruyama, K.; Mataga, N.; Asahi, T.; Yamazaki, I.; Tamai, N. *J. Am. Chem. Soc.* **1990**, *112*, 4958.

(16) Sessler, J. L.; Johnson, M. R.; Lin, T.-Y.; Creager, S. E. *J. Am. Chem. Soc.* **1988**, *110*, 3659.

10.1021/ja9900454 CCC: $19.00 
Published on Web 02/24/2000

reorganization energy, temperature, and electronic coupling have so far been well analyzed. However, serious limitation is inherent in model compounds. In such models a spacer is inevitably used to fix a redox pair, but the spacer itself takes part in ET. It is generally accepted that ET in linked model systems takes place much faster than that in protein[7a,27] due to the "through-bond" or superexchange mechanism.[28] Therefore, it is believed that synthetic models are not well suitable for the study of ET pathways in biological systems, where a donor and an acceptor are embedded in protein without direct chemical bonds. To enhance "through-space" and solvent-mediated pathways against "through-bond" ones in synthetic models, several clamp and U-shaped (donor)−(rigid spacer)−(acceptor) molecules have been synthesized.[29] We have also prepared porphyrin−spacer−benzoquinone molecules, where the spacer is spiro[4.4]nonane and a phenyl group is inserted covalently between the intervening space of the redox pair.[30] It was initially intended for such models to clarify the contribution of the inserted $\pi$-system as a stepping stone in "through-space" pathways between a donor and an acceptor upon ET. However, it was found that the "through-bond" pathways are much more effective compared with the "through-space" ones. In addition, the model in which a phenyl group locates outside of the space between the redox pair has larger rates of ET by a factor of 2−3 than those of the models, where a phenyl group locates inside of the space between the redox pair or no phenyl group is present. Thus, it seems quite difficult to evaluate the effect of chemical bonds between a redox pair accurately. This is because in model systems the change of linking bonds inevitably results in the structural and orbital change, which is in sharp contrast with the biological situation where a donor and an acceptor are not linked completely by chemical bonds. Due to these difficulties, the contribution of the different kinds of chemical bonds upon ET has not been well understood.[31] For the evaluation of such an effect we designed and synthesized compounds **1**, where a three-membered ring is introduced into the *trans*-decalin spacer of **2** (Figure 1).[17] Since the same redox pair is employed to connect the donor and acceptor with the

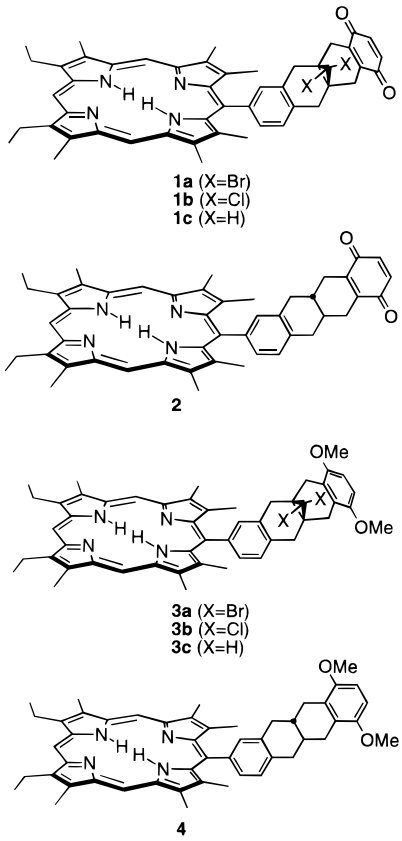


**Figure 1.** Molecular structures of **1**−**4**.

(17) (a) Sakata, Y.; Nakashima, S.; Goto, Y.; Tatemitsu, H.; Misumi, S.; Asahi, T.; Hagihara, M.; Nishikawa, S.; Okada, T.; Mataga, N. *J. Am. Chem. Soc.* **1989**, *111*, 8979. (b) Sakata, Y.; Tsue, H.; Goto, Y.; Misumi, S.; Asahi, T.; Nishikawa, S.; Okada, T.; Mataga, M. *Chem. Lett.* **1991**, 1307. (c) Tsue, H.; Nakashima, S.; Goto, Y.; Tatemitsu, H.; Misumi, S.; Abraham, R. J.; Asahi, T.; Tanaka, Y.; Okada, T.; Mataga, N.; Sakata, Y. *Bull. Chem. Soc. Jpn.* **1994**, *67*, 3067. (d) Sakata, Y.; Tsue, H.; O'Neil, M. P.; Wiederrecht, G. P.; Wasielewski, M. R. *J. Am. Chem. Soc.* **1994**, *116*, 6904. (e) Sakata, Y.; Imahori, H.; Tsue, H.; Higashida, S.; Akiyama, T.; Yoshizawa, E.; Aoki, M.; Yamada, K.; Hagiwara, K.; Taniguchi, S.; Okada, T. *Pure Appl. Chem.* **1997**, *69*, 1951.

(18) Isied, S. S.; Ogawa, M. Y.; Wishart, J. F. *Chem. Rev.* **1992**, *92*, 381.

(19) (a) Gray, H. B. *Chem. Soc. Rev.* **1986**, *15*, 17. (b) Mayo, S. L.; Ellis, W. R., Jr.; Crutchley, R. J.; Gray, H. B. *Science* **1986**, *233*, 948. (c) Winkler, J. R.; Gray, H. B. *Chem. Rev.* **1992**, *92*, 369.

(20) Peterson-Kennedy, S. E.; McGourty, J. L.; Ho, P. S.; Sutoris, C. J.; Liang, N.; Zemel, H.; Blough, N. V.; Margoliash, E.; Hoffmann, B. M. *Coord. Chem. Rev.* **1985**, *64*, 125.

(21) (a) McLendon, G. *Acc. Chem. Res.* **1988**, *21*, 160. (b) McLendon, G.; Hake, R. *Chem. Rev.* **1992**, *92*, 481.

(22) (a) Schanze, K. S.; Sauer, K. *J. Am. Chem. Soc.* **1985**, *110*, 1180. (b) Schanze, K. S.; Cabana, L. A. *J. Phys. Chem.* **1990**, *94*, 2740.

(23) (a) Pöllinger, F.; Musewald, C.; Heitele, H.; Michel-Beyerle, M. E.; Anders, C.; Futscher, M.; Voit, G.; Staab, H. A. *Ber. Bunsen-Ges.* **1996**, *100*, 2076. (b) Häberle, T.; Hirsch, J.; Pöllinger, F.; Heitele, H.; Michel-Beyerle, M. E.; Anders, C.; Döhling, A.; Krieger, C.; Rückemann, A.; Staab, H. A. *J. Phys. Chem.* **1996**, *100*, 18269.

(24) (a) DeGraziano, J. M.; Macpherson, A. N.; Liddell, P. A.; Noss, L.; Sumida, J. P.; Seely, G. R.; Lewis, J. E.; Moore, A. L.; Moore, T. A.; Gust, D. *New J. Chem.* **1996**, *20*, 839. (b) Kuciauskas, D.; Liddell, P. A.; Hung, S.-C.; Lin, S.; Stone, S.; Seely, G. R.; Moore, A. L.; Moore, T. A.; Gust, D. *J. Phys. Chem. B* **1997**, *101*, 429.

(25) Harriman, A.; Odobel, F.; Sauvage, J.-P. *J. Am. Chem. Soc.* **1995**, *117*, 9461.

(26) (a) Imahori, H.; Hagiwara, K.; Aoki, M.; Akiyama, T.; Taniguchi, S.; Okada, T.; Shirakawa, M.; Sakata, Y. *J. Am. Chem. Soc.* **1996**, *118*, 11771. (b) Imahori, H.; Hagiwara, K.; Akiyama, T.; Aoki, M.; Taniguchi, S.; Okada, T.; Shirakawa, M.; Sakata, Y. *Chem. Phys. Lett.* **1996**, *263*, 545. (c) Williams, R. M.; Koeberg, M.; Lawson, J. M.; An, Y.-Z.; Rubin, Y.; Paddon-Row, M. N.; Verhoeven, J. W. *J. Org. Chem.* **1996**, *61*, 5055. (d) Imahori, H.; Yamada, K.; Hasegawa, M.; Taniguchi, S.; Okada, T.; Sakata, Y. *Angew. Chem., Int. Ed. Engl.* **1997**, *36*, 2626. (e) Liddell, P. A.; Kuciauskas, D.; Sumida, J. P.; Nash, B.; Nguyen, D.; Moore, A. L.; Moore, T. A.; Gust, D. *J. Am. Chem. Soc.* **1997**, *119*, 1400. (f) Imahori, H.; Ozawa, S.; Ushida, K.; Takahashi, M.; Azuma, T.; Ajavakom, A.; Akiyama, T.; Hasegawa, M.; Taniguchi, S.; Okada, T.; Sakata, Y. *Bull. Chem. Soc. Jpn.* **1999**, *72*, 485. (g) Tamaki, K.; Imahori, H.; Nishimura, Y.; Yamazaki, I.; Shimomura, A.; Okada, T.; Sakata, Y. *Chem. Lett.* **1999**, 227. (h) Tamaki, K.; Imahori, H.; Nishimura, Y.; Yamazaki, I.; Sakata, Y. *Chem. Commun.* **1999**, 625. (i) Fujitsuka, M.; Ito, O.; Imahori, H.; Yamada, K.; Yamada, H.; Sakata, Y. *Chem. Lett.* **1999**, 721.

(27) (a) Oevering, H.; Verhoeven, J. W.; Paddon-Row, M. N.; Warman, J. M. *Tetrahedron* **1989**, *45*, 4751. (b) Jordan, K. D.; Paddon-Row, M. N. *Chem. Rev.* **1992**, *92*, 395. (c) Paddon-Row, M. N. *Acc. Chem. Res.* **1994**, *27*, 18. (d) Larsson, S.; Volosov, A. *J. Chem. Phys.* **1986**, *85*, 2548. (e) Moser, C. C.; Keske, J. M.; Warncke, K.; Fraid, R. S.; Dutton, P. L. *Nature* **1992**, *355*, 796.

(28) (a) McConnell, H. M. *J. Chem. Phys.* **1961**, *35*, 508. (b) Miller, J. R. *New J. Chem.* **1987**, *11*, 83. (c) Bixon, M.; Jortner, J. *J. Chem. Phys.* **1997**, *107*, 5154.

(29) (a) Lawson, J. M.; Paddon-Row, M. N.; Schuddeboom, W.; Warman, J. M.; Clayton, A. H. A.; Ghiggino, K. P. *J. Phys. Chem.* **1993**, *97*, 13099. (b) Kumar, K.; Lin, Z.; Waldeck, D. H.; Zimmt, M. B. *J. Am. Chem. Soc.* **1996**, *118*, 243. (c) Gosztola, D.; Wang, B.; Wasielewski, M. R. *J. Photochem. Photobiol. A* **1996**, *102*, 71. (d) Reek, J. N. H.; Rowan, A. E.; de Gelder, R.; Beurskens, P. T.; Crossley, M. J.; De Feyter, S.; de Schryver, F.; Nolte, R. J. M. *Angew. Chem., Int. Ed. Engl.* **1997**, *36*, 361. (e) Jolliffe, K. A.; Bell, T. D. M.; Ghiggino, K. P.; Langford, S. J.; Paddon-Row, M. N. *Angew. Chem., Int. Ed. Engl.* **1998**, *37*, 916. (f) Kumar, K.; Kurnikov, I. V.; Beratan, D. N.; Waldeck, D. H.; Zimmt, M. B. *J. Phys. Chem. A* **1998**, *102*, 5529. (g) Williamson, D. A.; Bowler, B. E. *J. Am. Chem. Soc.* **1998**, *120*, 10911.

(30) (a) Higashida, S.; Tsue, H.; Sugiura, K.; Kaneda, T.; Sakata, Y.; Tanaka, Y.; Taniguchi, S.; Okada, T. *Bull. Chem. Soc. Jpn.* **1996**, *69*, 1329. (b) Higashida, S.; Tsue, H.; Sugiura, K.; Kaneda, T.; Tanaka, Y.; Taniguchi, S.; Okada, T.; Sakata, Y. *Chem. Lett.* **1995**, 515.

**Scheme 1**

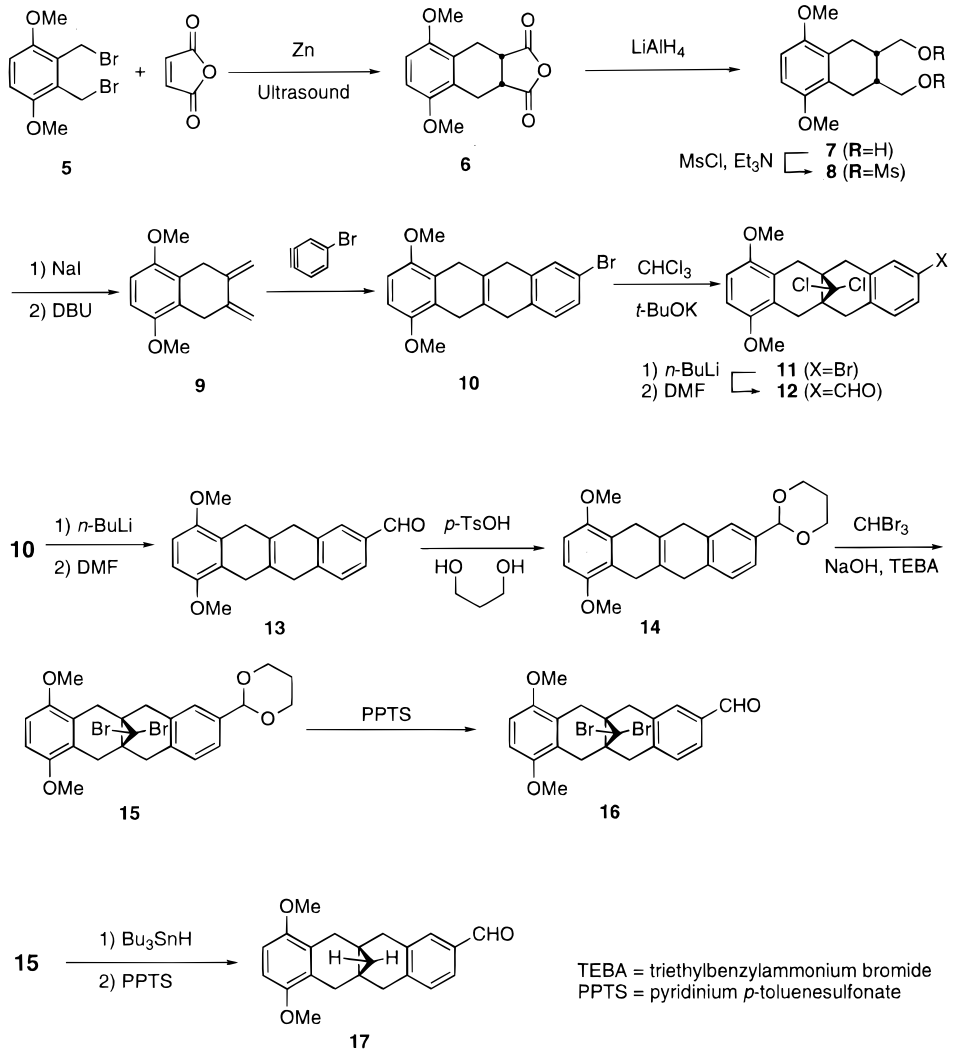


rigid spacer having the same number of intervening bonds, it is expected that the effect of the structural change in the spacer can be evaluated by comparing the ET rates of these two compounds.

## Results

**Synthesis.** The synthesis of **2** and the reference **4** was reported elsewhere.[17c] The preparation of **1** and the reference **3** was carried out as shown in Schemes 1 and 2. An important synthetic intermediate **10** was prepared by the Diels−Alder reaction of **5** with maleic anhydride in the presence of activated zinc powder, followed successively by reduction with $LiAlH_4$, mesylation of alcohol groups, treatment with NaI and DBU, and the Diels−Alder reaction of **9** with 4-bromobenzyne generated in situ. The synthesis of the spacer **12** having a dichlorocyclopropane ring was carried out by treatment of **10** with dichlorocarbene followed by formylation using BuLi and DMF. On the other hand, the synthetic route to the spacer **16** having dibromocyclopropane was slightly changed due to the low yield of the formylation reaction in the presence of the dihalosubstituted cyclopropane ring. Thus, **16** was prepared by formylation of **10**, followed successively by protection with the 1,3-dioxane ring, cyclopropanation, and deprotection. Moreover, a spacer **17** without halogen atoms on the cyclopropane ring was prepared from **15** using $Bu_3SnH$ and pyridinium *p*-toluenesulfonate (PPTS). The acid-catalyzed coupling reaction of tetrapyrrole **18**[32] with aldehydes **16**, **12**, and **17** in methanol gave porphyrins **3a**, **3b**, and **3c**, respectively (Scheme 2). The target compounds **1a** and **1b** were obtained by demethylation of **3a** and **3b** with $BBr_3$ in $CH_2Cl_2$, followed by oxidation with $PbO_2$. However, many attempts to convert **3c** to **1c** were unsuccessful due to the cleavage of the three-membered ring. The structures of the new compounds were determined on the basis of spectral data and elemental analysis (see Supporting Information).

**Scheme 2**

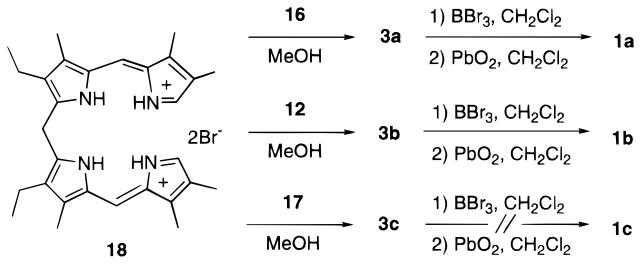


(31) (a) Heitele, H.; Michel-Beyerle, M. E. *J. Am. Chem. Soc.* **1985**, *107*, 8286. (b) Larson, S. L.; Hendrickson, S. M.; Ferrere, S.; Derr, D. L.; Elliott, C. M. *J. Am. Chem. Soc.* **1995**, *117*, 5881. (c) Osuka, A.; Tanaka, N.; Kawabata, S.; Yamazaki, I.; Nishimura, Y. *J. Org. Chem.* **1995**, *60*, 7177. (d) de Rege, P. J. F.; Williams, S. A.; Therien, M. J. *Science* **1995**, *269*, 1409. (e) Yamada, K.; Imahori, H.; Nishimura, Y.; Yamazaki, I.; Sakata, Y. *Chem. Lett.* **1999**, 895.

(32) Johnson, A. W.; Kay, I. T. *J. Chem. Soc.* **1965**, 1620.

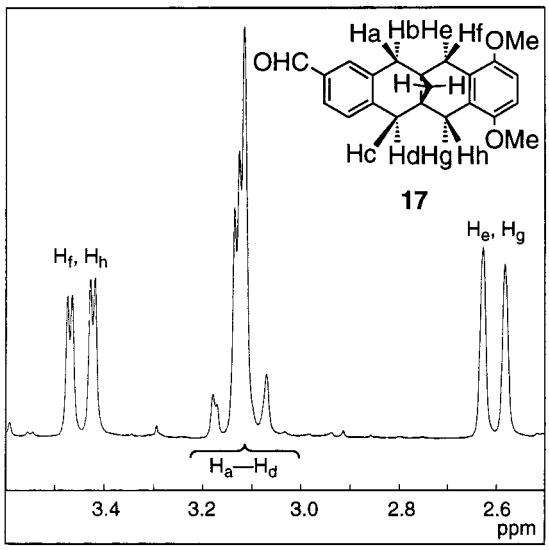


**Figure 2.** Enlarged $^1$H NMR spectra (360 MHz) of **17** in $CDCl_3$.

**Structure.** To get information on the precise structure of the spacers in **1** and **2**, $^1$H NMR analysis and theoretical calculations were carried out for the simplified model compounds of **1** and **2**. Figure 2 illustrates a small portion of $^1$H NMR spectra of **17**. The assignments of the peaks were done on the basis of NOE and decoupling technique. The peaks of $H_a$—$H_d$ in **17** constitute a higher-order pattern, while those of $H_e$—$H_h$ exhibit first-order splitting. The difference seems to originate from the difference in the magnetic environment of these protons. AM1 calculations of simplified model **19** with a three-membered ring revealed the existence of three stable conformers with similar lowest energies (Figure 3).[33] The conformer **20**-1 (heat of formation = 11.8 kcal mol$^{-1}$) has an extended geometry, while in conformers **20**-2 (12.1 kcal mol$^{-1}$) and **20**-3 (12.5 kcal mol$^{-1}$) either of the two six-membered rings of the tricyclo[4.4.1]-undecane framework is folded. Hayashi and Kato carried out ab initio calculations using the Hartree−Fock (HF) wave function with split valence 3-21G basis set to optimize the geometry of **19**.[34] They found two equilibrium geometries, **20**-1′ and **20**-3′, which are quite similar to **20**-1 and **20**-3. The energy calculated for the structure of **20**-1′ is slightly lower (1.1 kcal mol$^{-1}$) than that of **20**-3′. To evaluate the effect of basis set on the relative stability of **20**-1′ and **20**-3′, they repeated the HF calculations with the 6-31G* basis set at the 3-21G-optimized geometries. The resultant energy of **20**-1′ was slightly higher (3.3 kcal mol$^{-1}$) than that of **20**-3′. Considering the small barrier to inversion about two methylene carbons in the cyclohexene ring of **20**-1′ and **20**-3′, it was concluded that both conformations **20**-1′ and **20**-3′ exist in solution. Accordingly, the two conformations of the spacers **20**-1 and **20**-3 were used to examine the molecular structures of compound **1** in the following paragraph. On the other hand, in the $^1$H NMR spectrum of **21**, which was a synthetic intermediate of **2**,[17c] the vicinal coupling constant between $H_c$ and $H_d$ was deduced to be 14 Hz with the aid of the *J*-resolved spectrum (Figure 4).[17a] Therefore, the configuration of the decalin junction is concluded to be trans. MM2 calculation of simplified model **22** gave one stable conformer **23** (Figure 3). The dihedral angle of the two $\pi$ rings in **23** is 176°, indicating that the whole molecular structure is approximately planar. The geometry of **23** is quite similar to that of **23′**, which was optimized by Hayashi and Kato using similar ab initio calculations.[34]

Since the separation distance between donor and acceptor has been reported to play an important role in ET,[2] whole structures of compounds **24** and **25** were constructed using the optimized geometries of **20**-1, **20**-3, and **23** and a porphyrin unit to determine the distances between the chromophores.[17] In Figure 5, models **26**-1 and **26**-3 correspond to compound **1** with the extended (**20**-1) and folded (**20**-3) spacer frameworks, respectively. Besides, model **27** corresponds to **2** with the *trans*-decalin spacer (**23**). The dihedral angles between porphyrin and *meso*-phenyl rings were set to be 90° which has so far been determined experimentally.[17c] As summarized in Table 1, on the whole,

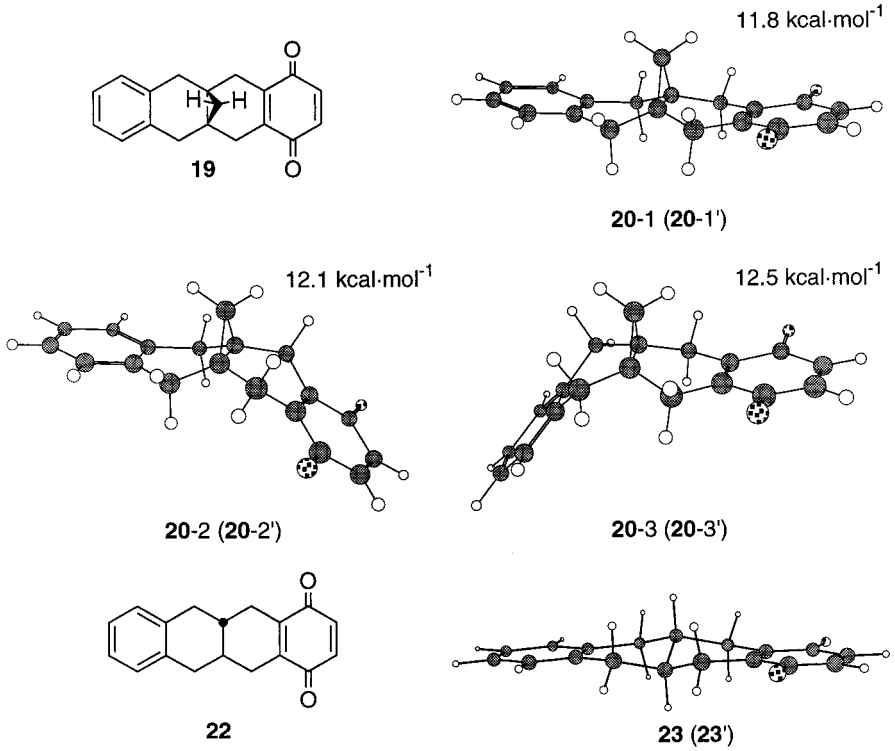


**Figure 3.** AM1- and MM2-minimized conformers (and their heats of formation) of **19** and **22**.

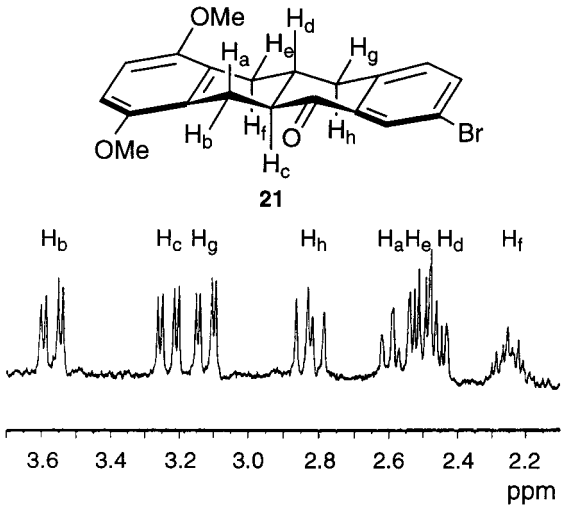


**Figure 4.** Enlarged $^1$H NMR spectra (360 MHz) of **21** in $CDCl_3$.

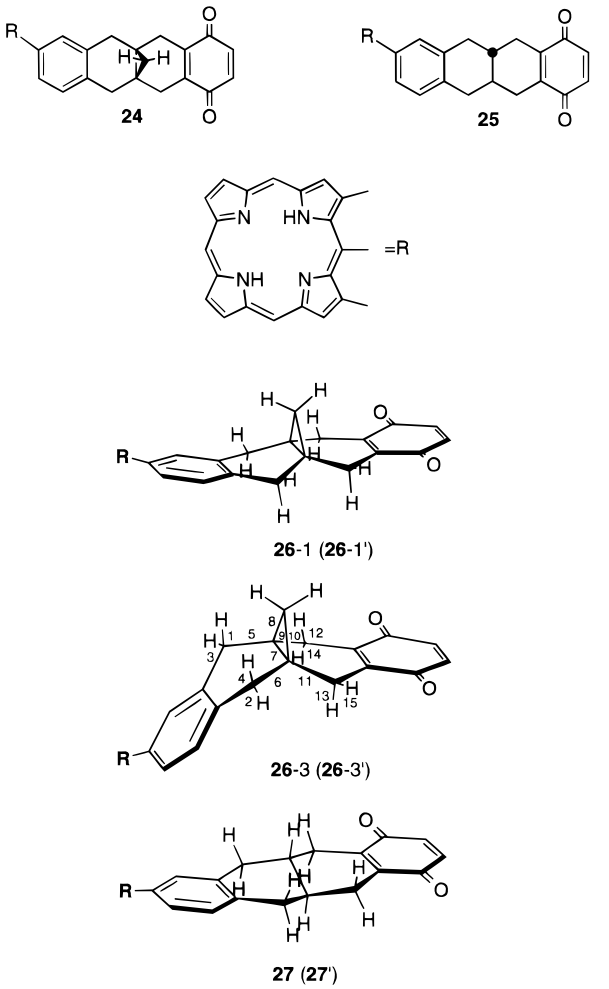


**Figure 5.** AM1-minimized conformers of **24** and **25**.

the separation distances between the redox pair in **26**-1 and **27** ($R_{cc}$ = 13.3 Å) were found to be nearly the same irrespective of both the structures and conformations of the spacers, while **26**-3 with the folded geometry has a slightly short distance ($R_{cc}$ = 12.2 Å). The structures of **26**-1, **26**-3, and **27** are quite consistent with those of **26**-1′, **26**-3′, and **27**′, calculated by Hayashi and Kato, using single-point HF/3-21G calculations.[34]

(33) Theoretical calculations were performed by using an ANCHOR2 molecular modeling system, Fujitsu Limited.

(34) Hayashi, S.; Kato, S. *J. Phys. Chem. A* **1998**, *102*, 2878.

**Table 1.** Separation Distances between Porphyrin and Quinone Moieties

| model | $R_{cc}$/Å[a] | $R_{ee}$/Å[b] |
|---|---|---|
| **26**-1 | 13.3 | 8.7 |
| **26**-3 | 12.2 | 7.4 |
| **27** | 13.3 | 8.8 |

[a] Center-to-center distance. [b] Edge-to-edge distance.

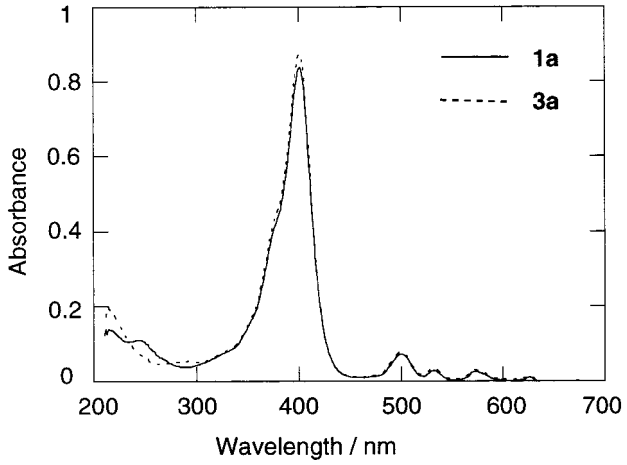


**Figure 6.** Electronic absorption spectra of **1a** and **3a** in THF ($5.0 \times 10^{-6}$ M).

**Photophysical and Redox Properties.** The electronic absorption spectra of **1** and **2** in THF are almost superimposable to those of the reference compounds **3** and **4** except for $\pi \rightarrow \pi^*$ transition of the quinone moiety at around 240 nm. A typical example is shown in Figure 6. The figure indicates that there is no special interaction between the porphyrin and quinone rings in **1** and **2** in the ground state and, hence, the ET rates can be obtained on the basis of the fluorescence lifetimes.

Steady-state fluorescence spectra of **1** and **2** in THF have the same band shape and peak positions ($\lambda_{em}$ = 629, 696 nm) as those of **3** and **4**. However, the fluorescence quantum yields are sharply reduced due to photoinduced intramolecular ET. The fluorescence lifetimes ($\tau$) of **1** and **2** were measured by a time-correlated single-photon-counting apparatus excited at 400 nm and monitored at 628 nm in THF and DMF. The decay curves of **1** and **2** could be fitted by two components. A typical example is shown for **1b** in THF in Figure 7. The major components (around 90%) are short and the minor ones (around 10%) have values quite close to those of the references without the quinone unit. Therefore, it seemed likely that the major components (Table 2) are related to intramolecular ET from the excited singlet state of the porphyrin to the quinone. The existence of halogen atoms causes in some cases the decrease of fluorescence lifetimes. For instance, the introduction of Cl or Br into a naphthalene moiety leads to the significant reduction of the fluorescence lifetimes,[35] i.e., 3.5 ns for 2-chloronaphthalene and 0.15 ns for 2-bromonaphthalene, with respect to 9.5 ns for naphthalene itself. However, such heavy atom effect can be discounted in **1a** and **1b** because $\tau$ values of **3a** and **3b** are quite similar to that of **4** as shown in Table 2.

As an example of the picosecond time-resolved transient absorption spectra, results of **1a** in THF are shown in Figure 8. Immediately after excitation with the 590 nm laser pulse, the $S_n \leftarrow S_1$ difference spectrum, characterized by the bleaching of the ground state porphyrin absorption at 500, 530, 575, and 630 nm of the Q-bands and strongly positive absorption at around

(35) Suppan, P. *Chemistry and Light*; The Royal Society of Chemistry: Cambrigde, 1994; pp 69.

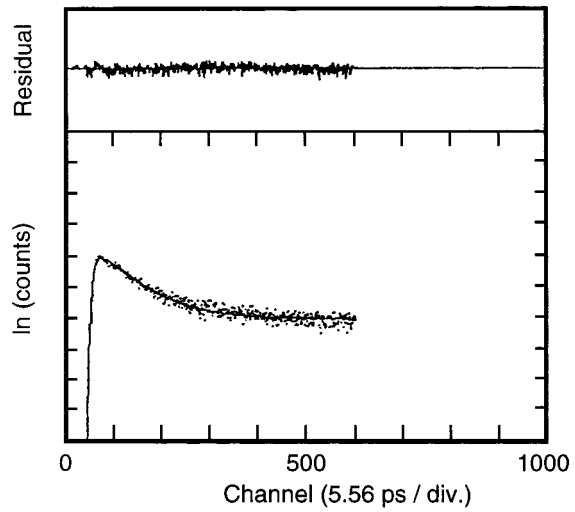


**Figure 7.** Fluorescence decay profile of **1b** in THF monitored at 628 nm ($\lambda_{ex} = 400$ nm). The top graph gives the residual to the biexponetial fit that is indicated by the solid line.

**Table 2.** Fluorescence Lifetimes and ET Rate Constants of **1**−**4** in THF and DMF

| | THF | | DMF | |
|---|---|---|---|---|
| compd | $\tau$/ns | $k_{et}$/s$^{-1}$ (rel ratio) | $\tau$/ns | $k_{et}$/s$^{-1}$ (rel ratio) |
| **1a** | 0.26 | $3.8 \times 10^9$ (58) | *a* | |
| **1b** | 0.34 | $2.9 \times 10^9$ (45) | 0.52 | $1.9 \times 10^9$ (22) |
| **2** | 8.2 | $6.5 \times 10^7$ (1) | 6.9 | $8.7 \times 10^7$ (1) |
| **3a** | 16.2 | | *a* | |
| **3b** | 15.3 | | 16.9 | |
| **4** | 17.4 | | 17.3 | |

[a] Not measured.

400−500 nm, and the stimulating emission at 700 nm were seen. However, along with the decay of the strong band at around 400−500 nm as well as the recovery of the bleaching, no appreciable transient absorption due to the porphyrin cation radical (∼700 nm) and the quinone anion radical were observed,[17] indicating that the recombination rate of the ion pair is much faster than the rate of the photoinduced charge separation under these conditions.[36] The fluorescence lifetimes are in good agreement with the lifetimes of the excited singlet states ($\tau = 340$ ps), which were determined by analyzing the time dependence of the transient $S_n \leftarrow S_1$ spectra (Figure 8). Although the presence of either of the radical ions could not be confirmed using the transient absorption spectroscopy, it is concluded, based on the related earlier work,[17] that the fluorescence quenching observed is a consequence of photoinduced ET from the excited singlet state of the porhyrin to the quinone. The forward ET rates ($k_{et}$) of **1** and **2** were calculated by the equation, $k_{et} = 1/\tau - 1/\tau_0$, where $\tau$ and $\tau_0$ are the lifetimes of **1** and **2** and of the reference compounds **3** and **4**, respectively. The results are summarized in Table 2. The ET rates of **1a** and **1b** were 58 and 45 times larger than that of **2** in THF, respectively, while in DMF that of **1b** was larger by a factor of 22 compared with that of **2**.

Redox potentials of **1** and **2** were obtained by differential pulse voltammetry (DPV) in dichloromethane containing 0.1 M *n*-$Bu_4NClO_4$ (Table 3). The values of the DPV peak potentials were used to calculate the free energy changes ($-\Delta G°$) for the ET reaction of **1** and **2** in THF and DMF using

$$-\Delta G° = E_0 - (E_{ox} - E_{red}) - e^2/(4\pi\epsilon_0)\{[1/(2R^+) + 1/(2R^-) - 1/R_{cc}](1/\epsilon_s) - [1/(2R^+) + 1/(2R^-)](1/\epsilon_s')\} \quad (1)$$

(36) (a) Mataga, N.; Karen, A.; Okada, T.; Nishitani, S.; Sakata, Y.; Misumi, S. *J. Phys. Chem.* **1988**, *88*, 4650. (b) Frey, W.; Klann, R.; Laermer, F.; Elsaesser, T.; Baumann, E.; Futscher, M.; Staab, H. A. *Chem. Phys. Lett.* **1992**, *190*, 567. (c) Heitele, H.; Pöllinger, F.; Kremer, K.; Michel-Beyerle, M. E.; Futscher, M.; Voit, G.; Weiser, J.; Staab, H. A. *Chem. Phys. Lett.* **1992**, *188*, 270. (d) Hung, S.-C.; Lin, S.; Macpherson, A. N.; DeGraziano, J. M.; Kerrigan, P. K.; Liddell, P. A.; Moore, A. L.; Moore, T. A. *J. Photochem. Photobiol. A: Chem.* **1994**, *77*, 207.

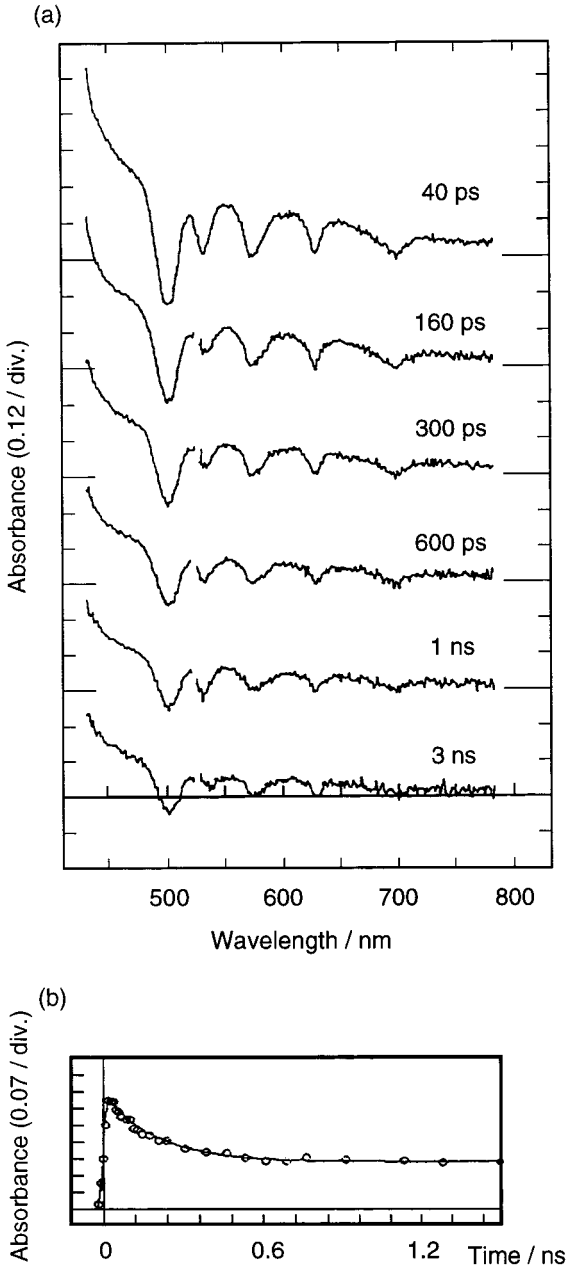


**Figure 8.** Picosecond time-resolved absorption spectra of **1a** in THF excited at 590 nm (a) and time dependence of the absorbance at 445 nm (b). The solid line is a simulated curve using $\tau = 340$ ps.

**Table 3.** Redox Potentials in $CH_2Cl_2$ and Free Energy Changes for ET Reaction of **1** and **2** in THF and DMF at 298 K

| | | | $-\Delta G°$/eV | | | |
|---|---|---|---|---|---|---|
| compd | $E_{ox}$/V | $E_{red}$/V | THF | | DMF | |
| **1a** | 0.88 | −0.49 | 0.67[a] | (0.68)[b] | 0.89[a] | (0.90)[b] |
| **1b** | 0.88 | −0.51 | 0.69[a] | (0.70)[b] | 0.91[a] | (0.92)[b] |
| **2** | 0.87 | −0.52 | 0.66 | | 0.89 | |

[a] Calculated for the extended conformation. [b] Calculated for the folded conformation.

**Table 4.** Static Dielectric Constants, Optical Dielectric Constants, Free Energy Changes, Reorganization Energies, Activation Energies, and ET Rate Constants as a Function of Temperature for **1a** and **2** in MTHF

| | | | $-\Delta G°$/eV | | | $\lambda$(theor)/eV[d] | | | $\Delta G°$ (theor)/eV | | | $k_{et}/s^{-1}$ | |
|---|---|---|---|---|---|---|---|---|---|---|---|---|---|
| $T$/K | $\epsilon_s$[a] | $\epsilon_{op}$[a] | **1a**[b] | **1a**[c] | **2** | **1a**[b] | **1a**[c] | **2** | **1a**[b] | **1a**[c] | **2** | **1a** | **2** |
| 293 | 7.009 | 1.9793 | 0.64 | 0.66 | 0.64 | 0.979 | 0.944 | 0.979 | 0.0286 | 0.0216 | 0.0293 | $1.7 \times 10^9$ | $2.8 \times 10^7$ [e] |
| 288 | 7.100 | 1.9817 | 0.65 | 0.66 | 0.64 | 0.982 | 0.946 | 0.982 | 0.0283 | 0.0213 | 0.0290 | *f* | $2.5 \times 10^7$ |
| 275 | 7.357 | 1.9878 | 0.66 | 0.67 | 0.65 | 0.989 | 0.953 | 0.989 | 0.0275 | 0.0207 | 0.0282 | $9.2 \times 10^8$ | *f* |
| 260 | 7.699 | 1.9948 | 0.67 | 0.68 | 0.67 | 0.998 | 0.962 | 0.998 | 0.0266 | 0.0200 | 0.0273 | *f* | $2.1 \times 10^7$ |
| 250 | 7.959 | 1.9996 | 0.68 | 0.69 | 0.68 | 1.00 | 0.968 | 1.00 | 0.0261 | 0.0195 | 0.0267 | $8.1 \times 10^8$ | *f* |
| 240 | 8.250 | 2.0043 | 0.69 | 0.70 | 0.69 | 1.01 | 0.975 | 1.01 | 0.0255 | 0.0190 | 0.0261 | *f* | $1.5 \times 10^7$ |
| 225 | 8.758 | 2.0114 | 0.71 | 0.72 | 0.70 | 1.02 | 0.986 | 1.02 | 0.0246 | 0.0183 | 0.0252 | $9.3 \times 10^8$ | *f* |
| 220 | 8.950 | 2.0138 | 0.71 | 0.72 | 0.71 | 1.03 | 0.989 | 1.03 | 0.0243 | 0.0181 | 0.0250 | *f* | $8.5 \times 10^6$ |
| 200 | 9.872 | 2.0232 | 0.73 | 0.74 | 0.73 | 1.04 | 1.01 | 1.04 | 0.0231 | 0.0172 | 0.0238 | $6.2 \times 10^8$ | $6.8 \times 10^6$ |

[a] Data from refs 38d and 39. [b] Calculated for the extended conformation. [c] Calculated for the folded conformation. [d] $\lambda$ ($=\lambda_s + \lambda_i$) was obtained from eq 3 with $\lambda_i = 0.2$ eV. [e] Extrapolated using eq 4. [f] Not measured.

where $E_{ox}$ and $E_{red}$ are the first oxidation potential of the porphyrin and the first reduction potential of the quinone in $CH_2Cl_2$, respectively, $R^+ = 5.5$ Å and $R^- = 3.75$ Å are the radii of the porphyrin and quinone rings, respectively, and $R_{cc}$ is the center-to-center distance between the two chromophores (Table 1). The level of the excited singlet state ($E_0$) in THF and DMF was estimated from the electronic absorption and fluorescence spectra to be 1.98 eV. The $E_{ox} - E_{red}$ values in THF ($\epsilon_s = 7.58$) and DMF ($\epsilon_s = 36.7$) were calculated using the redox potentials in $CH_2Cl_2$ ($\epsilon_s' = 8.93$). The calculated $-\Delta G°$ values for **1** and **2** in THF and DMF at 298 K are summarized in Table 3. The table shows that the free energy changes for the intramolecular ET of **1** and **2** are almost the same in both THF and DMF.

**Temperature Dependence of ET.** To obtain further information on the ET process, the $k_{et}$ constants of **1a** and **2** were measured as a function of temperature (200 to 300 K) using a time-correlated single-photon-counting technique in 2-methyltetrahydrofuran (MTHF). At all temperatures both compounds showed biexponential fluorescence decay curves, of which short components were used to estimate $k_{et}$ at relevant temperatures (Table 4) in a manner identical with that mentioned in the preceding section. For analyzing the ET reaction of **1a** and **2**, various factors controlling ET in the semiclassical Marcus equation[37] were determined:

$$k_{et} = \kappa_{el}\nu_n\kappa_n = 2\pi^{3/2}/[h(\lambda k_B T)^{1/2}]|V|^2 \exp[-(\Delta G° + \lambda)^2/(4\lambda k_B T)] = 2\pi^{3/2}/[h(\lambda k_B T)^{1/2}]|V|^2 \exp[-\Delta G^{\#}/(k_B T)] \quad (2)$$

where

$$\kappa_{el}\nu_n = 2\pi^{3/2}/[h(\lambda k_B T)^{1/2}]|V|^2; \quad \kappa_n = \exp[-\Delta G^{\#}/(k_B T)]; \; \Delta G^{\#} = (\Delta G° + \lambda)^2/(4\lambda)$$

In the eq 2, $\kappa_{el}$ and $\kappa_n$ are the electronic and nuclear factors, $\nu_n$ is the frequency of nuclear motion through the transition state, $h$ is the Planck constant, $|V|$ is the electronic coupling matrix element (ECE), $\lambda$ is the reorganization energy, $k_B$ is the Boltzmann constant, $T$ is absolute temperature, $-\Delta G°$ is the Gibbs energy change for the ET reaction, and $\Delta G^{\#}$ is the Gibbs activation energy in Marcus theory.

First, the free energy changes ($-\Delta G°$) of **1a** and **2** in MTHF were estimated on the basis of eq 1 (Table 4). Second, total reorganization energy ($\lambda = \lambda_i + \lambda_s$) was divided into an internal term $\lambda_i$ involving vibrational energy changes between the reactant and product states and a solvent term $\lambda_s$ involving the solvent orientation and polarization. The former was assumed to be 0.2 eV which was reported for similar porphyrin−quinone dyads as a reasonable value,[38a−d] whereas the solvent dependence of the latter was calculated by

$$\lambda_s = e^2/(4\pi\epsilon_0)[1/(2R^+) + 1/(2R^-) - 1/R_{cc}][1/\epsilon_{op} - 1/\epsilon_s] \quad (3)$$

where $R^+$, $R^-$, and $R_{cc}$ are the same values as those used for estimation of $-\Delta G°$ in THF and DMF, and $\epsilon_{op}$ and $\epsilon_s$ are the optical and static dielectric constants of the surrounding medium.[38d,39] Inserting these values into eqns 1−3 yielded almost equal values of $-\Delta G°$ and $\lambda$ for **1a** and **2**, whereas the values of $\Delta G^{\#}$ for **1a** with the folded conformation are significantly smaller than those of **1a** with the extended conformation and **2**, as summarized in Table 4. Finally, the Marcus eq 2 was reduced to the linearized form as given in the eq 4 for the evaluation of ECE $|V|$ in **1a** and **2**.

$$\ln(k_{et}T^{1/2}) = \ln\{2\pi^{3/2}|V|^2/[h(\lambda k_B)^{1/2}]\} - (\Delta G° + \lambda)^2/(4\lambda k_B T) = \ln\{2\pi^{3/2}|V|^2/[h(\lambda k_B)^{1/2}]\} - \Delta G^{\#}/(k_B T) \quad (4)$$

According to eqs 1−3, photoinduced ET in **1a** and **2** should have a significant driving force in solvents of medium and high polarity and fulfilll the "normal" region condition that $-\Delta G° < \lambda$, while the barrier is relatively small. Figure 9 shows Arrhenius plots of the ET rates of **1a** and **2** against the reciprocal of absolute temperature. The plots show no appreciable systematic deviation from the best fit straight line. $|V|$ and $\lambda$, deduced from the intercept and the slope, respectively, were calculated to be 6.2 $cm^{-1}$ (or 6.3 $cm^{-1}$ for the bended conformer) and 1.12 eV (or 1.14 eV for the bended conformer) for **1a** and 2.1 $cm^{-1}$ and 1.33 eV for **2** (Table 5). The values of $|V|$ for **1a** are larger by a factor of about 3 compared with that of **2**, while those of $\lambda$ for **1a** are smaller by about 0.2 eV than that of **2**. These results clearly demonstrate that both $V$ and $\lambda$ are different for **1a** and **2**, despite the $-\Delta G°$ for the ET and the separation distance and the number of intervening bonds between the redox pair being quite similar. In addition, there is a discrepancy

(37) (a) Marcus, R. A. *J. Chem. Phys.* **1965**, *43*, 679. (b) Marcus, R. A. *J. Chem. Phys.* **1956**, *24*, 966.

(38) (a) Archer, M. D.; Gadzekpo, V. P. Y.; Bolton, J. R.; Schmidt, J. A.; Weedon, A. C. *J. Chem. Soc., Faraday Trans. 2* **1986**, *82*, 2305. (b) Rempel, U.; Von Maltzan, B.; Von Borczykowski, C. *Z. Phys. Chem.* **1991**, *170*, 107. (c) Gaines, G. L., III; O'Neil, M. P.; Svec, W. A.; Niemczyk, M. P.; Wasielewski, M. R. *J. Am. Chem. Soc.* **1991**, *113*, 719. (d) Liu, J.-y.; Bolton, J. R. *J. Phys. Chem.* **1992**, *96*, 1718. (e) Zeng, Y.; Zimmt, M. B. *J. Phys. Chem.* **1992**, *96*, 8395. (f) Kroon, J.; Oevering, H.; Verhoeven, J. W.; Warman, J. M.; Oliver, A. M.; Paddon-Row, M. N. *J. Phys. Chem.* **1993**, *97*, 5065.

(39) Furutsuka, T.; Imura, T.; Kojima, T.; Kawabe, K. *Technol. Rep. Osaka University* **1974**, *24*, 367.

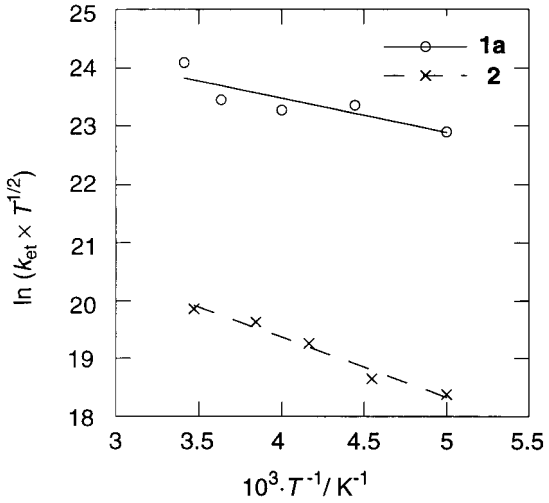


**Figure 9.** Arrhenius analyses of the temperature-dependent ET rate constants for **1a** and **2** in MTHF.

**Table 5.** Marcus Analysis of Temperature Dependence of $k_{et}$ for **1a** and **2** in MTHF According to Eq 4

| compd | slope/ K | intercept | r[a] | $\Delta G^{\#}$(expt)/ eV[b] | $\lambda$(expt)/ eV[b] | $\|V\|$(expt)/ cm$^{-1}$ [b] |
|---|---|---|---|---|---|---|
| **1a** | −588 | 25.8 | 0.862 | 0.0507 | 1.12[c] (1.14)[d] | 6.2[c] (6.3)[d] |
| **2** | −1049 | 23.6 | 0.986 | 0.0904 | 1.33 | 2.1 |

[a] Absolute value of the correlation coefficient. [b] Determined experimentally. [c] Calculated for the extended conformation. [d] Calculated for the bended conformation.

between the theoretical and experimetal reorganization energies as well as $\Delta G^{\#}$ (Tables 4 and 5), which will be discussed later.

## Discussion

ET rate constants for **1** and **2** were measured and analyzed using the semiclassical Marcus equation. No large solvent dependence of $k_{et}$ was observed for **1** and **2** in THF and DMF. These solvent effects can be qualitatively explained as follows. In general, as the solvent polarity increases, both the free energy gap for the photoinduced charge separation and the solvent reorganization energy increase. Thus, the solvent effect on $-\Delta G^{\circ}$ may be compensated for by the change in the overall reorganization energy.[11,12,40] Surprisingly, $k_{et}$ values of **1** with three-membered rings in the spacer are ca. 50 to 60 times (in THF) or ca. 20 times (in DMF) larger than that of **2** (Table 2). According to the Marcus theory,[37] $k_{et}$ is dominated by the electronic coupling matrix element $|V|$, reorganization energy $\lambda$, and free energy change $-\Delta G^{\circ}$ associated with the ET reaction. At 293 K the ratio of the ET rates for **1a** versus **2** in MTHF is estimated to be 61. Considering that the ratio of $|V|^2$-(**1a**)/$|V|^2$(**2**) = 8.4 for the extended conformation and 8.7 for the folded one, the different nuclear factor is contributing a factor of 7.3 and 7.0 to the kinetics, respectively, reaching almost 40% of the overall kinetics. Therefore, the observed large difference in $k_{et}$ for **1** and **2** should be attributed to the difference in both $|V|$ and $\lambda$, because $-\Delta G^{\circ}$ values were actually the same. More noteworthy is that the structural factors controlling ET, that is, separation distance and the number of the intervening bonds between the redox pair, are the same or almost the same for **1** and **2**. Therefore, the observed remarkable differences in the $|V|$ and $\lambda$ terms are most probably to due to the geometry and/or nature of the bonds in the spacer. We will present plausible explanations for the difference in both the $|V|$ and $\lambda$ for **1** and **2**.

Ab initio calculations on the ECE $|V|$ between the porphyrin and quinone moieties in the gas phase were carried out separately by Hayashi and Kato[34] for the optimized structures **26**-1′, **26**-3′, and **27**′, which are quite similar to **26**-1, **26**-3, and **27** (Figure 5). We will begin by recapitulating the previously reported results for **26**-1′, **26**-3′, and **27**′ (see the Supporting Information).

The overall ECEs $V_{RP}$ were calculated with the singly excited configuration interaction (SECI) matrix elements of intermediate states using the basis 1 and 2 spacer orbitals (Table 6). In constructing the reactant and product states, all the valence donor and acceptor $\pi^*$ orbitals and 11 and 4 $\pi^*$ orbitals of porphyrin and quinone were adopted. The energy levels of the reactant ($^1$P*-Q) and product (P$^{\bullet+}$($A_u$)-Q$^{\bullet-}$ and P$^{\bullet+}$($B_{1u}$)-Q$^{\bullet-}$) states as well as the resultant ECEs are summarized in Table 6. Although the excitation energies are overestimated by about 1 eV, the respective energies of the reactant and product states are similar for **26**-1′, **26**-3′, and **27**′. In the $A_u$ case, the ECEs with basis 1 and 2 were evaluated to be 6.27 and 6.57 cm$^{-1}$ for **27**′. These ECEs are slightly smaller than those for **26**-1′, 8.55 and 8.81 cm$^{-1}$, respectively. Considering that the relative position of the donor and acceptor parts in **26**-1′ is similar to that in **27**′, it seems likely that the presence of the cyclopropane ring in the spacer part does not cause the large difference in the magnitude of ECE. On the other hand, the ECEs for **26**-3′, 18.86 and 27.29 cm$^{-1}$ by basis 1 and 2, respectively, are much larger than those for **26**-1′ and **27**′. Accordingly, the large difference in the ECSs may be attributed to that in geometry between **26**-3′ and **27**′. For the $B_{1u}$ state, the ECEs for **26**-1′, **26**-3′, and **27**′ were calculated to be 6.45, 10.24, and 4.64 cm$^{-1}$ with basis 1, respectively. The relative magnitudes of these ECEs are in qualitative agreement with those in the $A_u$ case. In contrast, the ECEs for **26**-1′, **26**-3′, and **27**′ are similar using basis 2.

At the present it is impossible to perform similar ab initio calculations for **1a** and **1b** to obtain the ECEs for the ET reaction, because of the extraordinary calculation time. Hayashi and Kato assumed that the $k_{et}$ rate of **1c** is much larger than that of **2**, based on the fact that the $k_{et}$ rates of **1a** and **1b** are much larger than that of **2**. Thus, it was concluded tentatively that the $A_u$ type state for **26**-3′ is responsible for the actual ET process. Although the experimental $|V|$ values were about 1/3 of the theoretical ones, the relative magnitude (about 3−4-fold) of the calculated $|V|$ values for models **26**-3′ and **27**′ is in good agreement with those of the experimental $|V|$ values for **1a** and **2** (Tables 5 and 6). This suggests that the folded geometry such as **26**-3′ contributes much to the ET reaction in **1a**. As a result of the slightly short edge-to-edge distance between the chromophores in **26**-3 with the folded conformation (Table 1), through-space interaction arising from the direct overlap of their molecular orbitals is supposed to be enhanced in **1a**. However, through-space interaction is known to decay exponentially with respect to the separation distance between the donor and acceptor.[2,7,27a] Hence, through-space interaction in **2** with extended conformation would be reduced, so that alternative through-bond interaction appears to become a main participant in the ET in **2**. To support this hypothesis, the overall ECEs $V_{RP}$, defined by the sum of the through-space term $V_{RP}^{space}$ and the through-bond term $V_{RP}^{bond}$, were separated into these terms using the SECI matrix elements of intermediate states using the basis 1 and 2 space orbitals.[34]

The decomposition of overall ECEs revealed that the through-bond ECEs $V_{RP}^{bond}$ is dominant in all systems except for **26**-3′

(40) (a) Kroon, J.; Verhoeven, J. W.; Paddon-Row, M. N.; Oliver, A. M. *Angew. Chem., Int. Ed. Engl.* **1991**, *30*, 1358. (b) Macpherson, A. N.; Liddell, P. A.; Lin, S.; Noss, L.; Seely, G. R.; DeGraziano, J. M.; Moore, A. L.; Moore, T. A.; Gust, D. *J. Am. Chem. Soc.* **1995**, *117*, 7202.

**Table 6.** Excitation Energy of Reactant and Product States and Electronic Coupling Elements $V_{RP}$

| | | | | $V_{RP}$ ($V_{RP}^{bond} + V_{RP}^{space}$)/cm$^{-1}$ | | | |
|---|---|---|---|---|---|---|---|
| | excitation energy/eV | | | $A_u$ | | $B_{1u}$ | |
| compd | $^1$P*-Q | P$^{\bullet+}$($A_u$)-Q$^{\bullet-}$ | P$^{\bullet+}$($B_{1u}$)-Q$^{\bullet-}$ | basis 1 | basis 2 | basis 1 | basis 2 |
| **26**-1′ | 3.059 | 5.611 | 6.076 | 8.55 (6.27 + 2.28) | 8.81 (6.53 + 2.28) | 6.45 (5.98 + 0.47) | 8.88 (8.41 + 0.47) |
| **26**-3′ | 3.059 | 5.422 | 5.887 | 18.86 (9.24 + 9.62) | 27.29 (17.67 + 9.62) | 10.24 (10.85−0.61) | 7.38 (7.99−0.61) |
| **27**′ | 3.059 | 5.634 | 6.098 | 6.27 (5.13 + 1.14) | 6.57 (5.43 + 1.14) | 4.64 (3.68 + 0.96) | 8.38 (7.42 + 0.96) |

in the $A_u$ case, which is consistent with the hypothesis. Thus, the through-space contribution is 1/3 to 1/2 of $V_{RP}$ in **26**-3′, whereas these terms in the other cases are relatively small. $V_{RP}^{bond}[\pi^*(\text{benzene})]$ contributes mainly to $V_{RP}^{bond}$ and is much larger than $V_{RP}^{bond}[\sigma^*]$, showing the $\pi^*$ orbitals of benzene in the spacers provide main routes for ET in the present systems. It was also found that the $\sigma^*$ states of the dimethyl groups at the $\beta$ position of the porphyrin part also give large contributions to the through-bond ECEs for **26**-3′ in the $A_u$ case, while these are reduced in the $B_{1u}$ case.

To obtain more detailed information on the mechanism of the intramolecular ET process, the pathway analyses were performed only for the case of $A_u$.[34] The pathway analyses for **26**-3′ revealed that the intermediate state involving the C−H $\sigma^*$ orbitals (C−H 14 in Figure 5) strongly interacts with the states involving the $\sigma^*$ orbitals of the benzene part in the spacer and the C−H $\sigma^*$ orbitals in the methyl groups at the $\beta$ positions of the porphyrin part, respectively. On the other hand, a similar strong interaction is not seen for **26**-1′ and **27**′. Hayashi and Kato pointed out that for **26**-3′ this results from short distance and matched mutual orientation between the $\sigma^*$ bonds characterizing those intermediate states due to the bended geometry of the spacer part. Overall, they insisted that the bent geometry of the spacer enhances the ECE in **26**-3′. Based on their results, the acceleration effect of **1a** and **1b** against **2** may be ascribed to the bent geometry of the spacer in **1a** and **1b**.

There are numerous recent observations of large solvent dependence of ET rate constants and electronic coupling in (donor)−(rigid spacer)−(acceptor) molecules where the donor and acceptor are in reasonably close proximity.[29] Zimmt et al. reported the large and solvent dependent $|V|$ found for their C-clamp-shaped molecule.[29b,f,38e] They proposed that solvent-mediated superexchange coupling accounts for the observed solvent dependence. Verhoven and Paddon-Row et al. also concluded that through-solvent coupling is effective in their U-shaped (donor)−(spacer)−(acceptor) molecules.[29a,e,38f] Therefore, the effect of the solvent fluctuation is likely to be important in the present systems. Preliminary ab initio calculation of **2** involving acetonitrile as solvent suggested that the character of the ET pathway in the solvent-induced ECE is different from the ECE in the gas phase.[41] However, further extensive calculations of both **1** and **2** in acetonitrile, including the intramolecular conformation changes and vibrations of the dyads, could not be carried out because of the overdemand for calculation time. For this purpose, efficient methods would be required to reduce the time, and this will be a subject of future study.

There is an alternative explanation for the enhancement of the electronic coupling in **1a** and **1b**. Allan reported the presence of a very low lying antibonding orbital in cyclopropane (2.6 eV) compared to the typical orbitals of unstrained cycloalkanes (4−6 eV $\sigma^*$).[42] This orbital was assigned to an antibonding one with C−H character. Since the bond lengths of C−Br in **1a** and of C−Cl in **1b** are expected to be much longer than that of C−H in **1c**, the involvement of the weaker C−Cl and C−Br would induce greater spatial overlap of the C−Cl or C−Br antibonding orbitals with the antibonds of the benzene rings in the spacer. Alternatively, the substitution of electron-withdrawing groups such as halogen atoms may lower the energy level of the lowest unoccupied molecular orbital (LUMO). Therefore, the increased mixing pathway due to the existence of the dihalosubstituted cyclopropane ring explains the enhancement of the electronic coupling in **1a** and **1b**. To demonstrate this hypothesis, ab initio calculations on molecular orbitals (MP2/3-21G*) were carried for 1,1-dibromocyclopropane (**28a**), 1,1-dichlorocyclopropane (**28b**), and cyclopropane (**28c**).[43] The energies of highest occupied molecular orbital (HOMO) and LUMO are found to be −10.24 eV for **28a**, −11.03 eV for **28b**, and −11.33 eV for **28c** and 3.583 eV for **28a**, 4.412 eV for **28b**, and 7.471 eV for **28c**, respectively. These clearly show that the introduction of the heavy halogen atoms into the cyclopropane framework makes the energy of LUMO lower, which is quite consistent with the above explanation. The explanation agrees with the fact that the ET rate for **1a** is larger than that for **1b**. Owing to the synthetic reason, the $k_{et}$ rate of **1c** could not be obtained. Considering that the energy levels of P$^{\bullet+}$($A_u$)-Q$^{\bullet-}$ and P$^{\bullet+}$($B_{1u}$)-Q$^{\bullet-}$ are quite similar, there is an alternative possibility for Hayashi and Kato's calculations that P$^{\bullet+}$($B_{1u}$)-Q$^{\bullet-}$ contributes to the photoinduced ET process greatly in the present system. They displayed the energies of the valence unoccupied orbitals for both basis 1 and 2 sets for **26**-1′. In basis 1, there are two main peaks at the regions of 4−7 eV and 14−22 eV. The lower and higher energy peaks consist of the $\pi^*$ and $\sigma^*$ orbitals, respectively. For basis 2, an additional two peaks appeared at the regions centered at 10 and 13 eV. These orbitals were identified as the $\sigma^*$ orbitals of the C−H antibonding and C−C antibonding characters. As discussed before, introduction of halogen atoms would further lower the energies of the $\sigma^*$ orbitals of the C−H antibonding, resulting in the enhancement of the ECEs of **1a** and **1b** against **1c**. Assuming the $B_{1u}$ case with basis 2, the ECEs are quite similar for **26**-1′, **26**-3′, and **27**′ as shown in Table 6. If this is the case, the order of ET rates would be **1a** > **1b** ≫ **1c** ≈ **2**.

Surprisingly, we found that the reorganization energies of **1a** are smaller than that of **2** by ca. 0.2 eV. The smaller reorganization energies of **1a** also contribute to acceleration of the photoinduced ET in **1a** compared with **2** by a factor of ca. 8. The experimental values are different from the calculated ones by 0.1−0.3 eV. Using the experimental $\lambda$ and calculated $\lambda_s$ at 293 K, $\lambda_i$ are estimated to be 0.34 (extended conformation) and 0.40 (folded confomation) for **1a** and 0.55 for **2**, which are larger than the assumed value (0.2 eV) for $\lambda_i$. Since both the

(41) Hayashi, S.; Kato, S. *J. Phys. Chem. A* **1998**, *102*, 3333.

(42) Allan, M. *J. Am. Chem. Soc.* **1993**, *115*, 6418.

(43) Theoretical calculations were performed by using SPARTAN Version 5.0, Wavefunction, Inc., CA.

internal and solvent reorganization energies are considered to be controlled mainly by the porphyrin and quinone moieties, not the spacer one, the difference is striking. At the present, we have no reasonable explanation for the results, but it might be due to the interaction between the donor and/or the acceptor and the spacer containing the dihalosubstituted cyclopropane and/or the change in geometry accompanying charge separation.[44]

The result of this study demonstrates that the subtle structural change in the spacer exerts a large influence upon the photoinduced ET. The rate acceleration can be explained experimentally by the enhancement of the electronic coupling as well as the decrease of the reorganization energy. The former may be due to the enhancement of the through-space ET pathway arising from the bent geometry of the spacer and/or of the mixing pathway induced by a very low lying antibonding orbital in the dihalosubstituted cyclopropane, whereas there is no clear explanation for the latter effect. The present result will provide basic information for understanding ET in protein, where a redox pair is not connected completely by chemical bonds. It should be emphasized here that the elaborated models **1** and **2** made it possible to evaluate the contribution of the spacer structure upon ET accurately.

(44) Shephard, M. J.; Paddon-Row, M. N. *J. Phys. Chem. A* **1999**, *103*, 3347.

**Acknowledgment.** We are indebted to Prof. S. Kato and S. Hayashi for the information and discussions. We also thank Prof. S. Takamuku, Dr. A. Ishida, and Dr. V. V. Borovkov for the measurements of the temperature-dependent fluorescence lifetimes. This work was supported by Grant-in-Aids for COE Research and Scientific Research on Priority Area of Electrochemistry of Ordered Interfaces and Creation of Delocalized Electronic Systems from Ministry of Education, Science, Sports and Culture, Japan. Y.S. thanks the Mitsubishi Foundation for financial support.

**Supporting Information Available:** Experimental procedures for all new compounds (PDF). This material is available free of charge via the Internet at http://pubs.acs.org.

JA9900454